Experimental and CFD comparison of driver's thermal plume with classical air diffusers

Amaury Jamin [a], *Paul Alexandru* Danca [b], *Bart* Janssens [a], *Florin* Bode [b], Ilinca Nastase [b], Walter Bosschaerts [a].

[a] Department of Mechanical Engineering, Royal Military Academy, Brussels, Belgium, amaury.jamin@mil.be

[b] CAMBI Research Center, Building Services Faculty, Technical University of Civil Engineering of Bucharest, Bucharest, Romania, paul.danca@utcb.ro, ilinca.nastase@utcb.ro

[c] Department of Mechanical Engineering, Technical University of Cluj Napoca Cluj, Napoca, Romania florin.bode@termo.utcluj.ro

[d] Department of Renewable Energy Sources, National Institute for R&D in Electric, Engineering ICPE-CA, Bucharest, Romania, paul.danca@icpe-ca.ro

Abstract. In confined spaces, such as vehicle cabins, airflow is one of the most critical factors affecting thermal comfort and pollutant dispersion. To develop innovative and energy-efficient HVAC systems, a deep understanding of the jet flows' interaction from air diffusers on the thermal plume became essential to improve our knowledge of airflow patterns for optimizing ventilation system design, thermal comfort, and indirectly, energy efficiency. We have developed a 1:1 scale mock-up with transparent walls, replicating a Renault Megane's interior in a climatic chamber and associated complex numerical models. PIV and IR measurements were firstly performed for the pure thermal plume with a thermal manikin in a driver's seat in this 1:1 scale mock-up. The experimental and numerical results showed good agreement regarding ranges and distributions. This paper presents experimental and numerical comparisons performed without and with ventilation systems to evaluate this interaction for classical air diffusers as a part of our larger project. The flow structure in the car cabin is complicated with existing large- and small-scale vortices. With an active ventilation system, the thermal plume is stronger in front of the head, the opposite of what has previously observed back the head. The airflow moves forward along the ceiling. The presence of the steering wheel distorts the flow direction at the thigh level. The additional velocity field on convective upward velocity in the shoulders' region is caused by impinging jets from diffusers. The Coanda effect caused by the central diffuser's flow creates a nonuniform and asymmetrical air distribution in the shoulders' region. A qualitative comparison of the jets' velocity distributions shows that the velocities are more uniform with innovative LAG diffusers than with the classical ones. This shows clearly the benefits of passive flow mixing to improve the thermal sensation.

Keywords. Human thermal plume, jet flow, PIV, IR, car cabin ventilation, CFD modeling.
DOI: https://doi.org/10.34641/clima.2022.314

1. Introduction

In recent decades, thermal comfort and air quality for passengers with reduced energy consumption are among the automotive industry's leading research and development goals. Driver stress or fatigue, driver and passenger health, energy consumption, and emissions are parameters that significantly impact a comfortable thermal environment [1-2].

Controlling thermal conditions in the passenger compartment remains a challenge for engineers because the fast dynamic behaviour of these systems makes it difficult to predict the optimal parameters for achieving thermal comfort. The inhomogeneity of the surface temperature distribution due to thermal convection effects directly affects the airflow at the precise locations. Moreover, the airflow patterns and their effects on the thermal sensation should be studied in more detail in the future. Due to thermal gradients and the presence of the passengers, the overall flow path (convection effects) can deviate significantly from the direction predicted by the guided vanes of the air diffusers. Therefore, the airflow distribution is one of the most critical factors for thermal comfort and pollutant dispersion in car cabins [3-4]. Indeed, in car cabins, a deep understanding of airflow patterns is essential for removing excess heat and diluting contaminants [5], which results from the interaction between human airflows, mainly thermal plumes from passengers and conditioned air delivered by the air HVAC systems [6].

Therefore, to develop innovative and energy-efficient HVAC systems, a better understanding of the following phenomena could provide fundamental information for the optimization of the design of

these systems: i) human thermal plume; ii) airflow, especially in the vent outlet and jet stream areas; iii) interaction of the jet flow from classical or innovative air diffusers on the development process of the human thermal plume. In passenger compartments, human thermal plumes generated by body heat loss significantly impact passenger comfort, pollutant dispersion, and air quality. The cabin interior's geometry, the air vents' manufacture and location, the grid vanes' design, and the HVAC's flow parameters set affect strongly influence the airflow in the jet stream area. For designing a mixing ventilation system, thermal comfort, air quality and energy consumption are the crucial parameters. In fact, a high induction level is desirable in these ventilation systems, allowing optimal mixing of the ventilating jet with the ambient air. From previous research, the innovative idea was to introduce lobed geometries passive control for improving air diffusion in buildings and vehicles with 12 studies regarding different configurations in UTCB and the French university of La Rochelle. Optimizing the design of innovative air diffusers, such as lobed ailerons, orientable lobed spherical nozzles, and cross-shaped lobed perforated panels, with passive flow mixing to improve the thermal sensation of the occupants appeared as an efficient, cost-effective solution to reduce the energy consumption for conventional, electric, or hybrid vehicles using an intelligent air diffusion strategy [7-9].

This type of phenomenon can be investigated experimentally using many different measurement techniques. PIV, an optical flow visualization method, is the most suitable method for studying the human thermal plume air distribution [10-11], characterized by low-velocity fields and transient behaviour and the velocity distribution of jet streams (large-scale PIV) [4,12,13]. In PIV measurements, the main difficulty is maintaining thermal equilibrium and achieving the most homogeneous seeding particle concentration. However, the main limitations of the experimental investigation are the parametric study and the reproducibility of specific boundary conditions. Computational Fluid Dynamics (CFD) has become very powerful in the automotive industry because it can provide a large amount of information relatively quickly and at a relatively low cost. From a numerical point of view, the human thermal plume is one of the most difficult to be reproduced correctly due to its unstable nature governed by buoyancy forces. A key factor in numerical simulations is validating and verifying the computational data. When the human thermal plume interacts with other flows in the microenvironment of the human body, the validation or calibration of the models becomes even more complicated. This microenvironment is extremely confined inside a vehicle, with unevenly distributed surface temperatures and high velocities near the human body and its plume. In our effort to study and understand the influence of air distribution in the car cabin on the thermal sensation of the human body, complex numerical models are developed.

To this end, we have developed a full-scale experimental model of a vehicle cabin that replicates the interior of a Renault Megane, with a real dashboard and associated air distribution system and real seats (see Fig. 1). This model -mostly transparent- allows the investigation of the involved flows through optical methods of measurements. In a previous study [14], we performed PIV and IR measurements of the thermal plume of a sophisticated Thermal Manikin (TM) in the driver's seat in a 1:1 scale mock-up of a Renault Megane car cabin in a climatic chamber where all active walls with surface temperatures controlled by a hydraulic and automation system were set up at constant temperature and without a ventilation system to validate the numerical model. Two conditions were checked to capture the pure thermal plume air distribution without ventilation. First, the new thermal equilibrium of the cabin must be achieved without any internal thermal energy being extracted by the A660 A/C laboratory unit. Secondly, the momentum of the seeding airflow introduced in the cabin mock-up must be negligible compared to the thermal plume [15]. Case 1 (without ventilation) was made to improve the understanding of this phenomenon separately in a confined space as a reference.

The results obtained with both methods showed good agreement regarding ranges and distributions of velocity and temperature in the sagittal and coronal planes [16-18]. The paper presents the experimental and numerical comparisons performed with no active and active ventilation system intended to evaluate the interaction of the jet flow from a classical vehicle air diffuser on the development process of the human thermal plume in the sagittal and coronal planes as the first step in our global plane. In the current literature, for the first time, the thermal plume of a seated person inside a vehicle is captured by optical measurement methods and compared with numerical models without (case 1) and with (case 2) ventilation systems from a classical air diffuser.

2. Experimental setup

A full-scale experimental model (see Fig. 1) was set up in an environmental chamber measuring 2.5 x 3.6 x 3.6 m, which is equipped with active walls and whose surface temperature is controlled by a hydraulic and automatic system for PIV and IR measurements. All active walls were set up at 20°C to have a constant temperature with an active ventilation system in the climatic chamber. An A660 A/C laboratory unit was used to control the injected air's mass flow, temperature, and humidity into the car cabin. The total volume flow rate was 191.3 m^3/h. A nude TM with a neuro-fuzzy control system named Suzi [19], characterized by a standard human size of 1.7 m and a total surface of 1.8 m^2 was used to generate the thermal plume's flow. A uniform body surface temperature of 34°C was imposed over the entire TM because it is easier to capture the thermal plume than a nonuniform surface temperature. The

TM is controlled by in-house software in LabVIEW based on a neuro-fuzzy system, allowing the user to specify setpoints for each of the 79 areas of surface temperature.

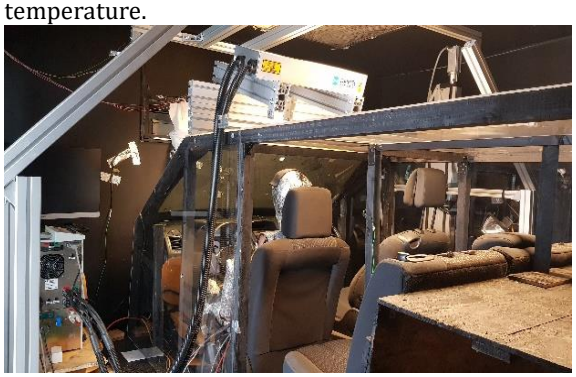

Fig. 1 – Experimental setup – 1:1 scale cabin mock-up with transparent walls.

The monitoring system can record the temperature evolution of the 395 available temperature sensors, 5 sensors in each of the 79 zones, and record the power consumption of each segment. Non-reflecting painting and material were used to mask all reflecting surfaces inside the cabin.

PIV measurements were carried out in a climatic chamber, using a TM in the driver's place inside the scale 1:1 mock-up. The purpose of PIV measurements was to experimentally verify the CFD velocity distribution around the TM's head (See Fig. 3: green planes) and CFD jet velocity distribution in the middle plane of air diffusers (See Fig. 3: blue planes). A PIV system, composed of a FlowSense EO camera with 2048x2048px as spatial resolution combined with a 50 mm lens and a Dual Power green (532 nm) Litron laser with an energy of 200 mJ, was used to measure the thermal plume and jet velocity profile. The maximum trigger rate of the PIV system between two pairs of images was 7.5 Hz. The time between pulses was 500-2000 μs, with 500 images for the thermal plume and 150-250 μs, with 250 images for the jet flow acquired for each measurement. The vehicle cabin was seeded with a high-volume liquid seeding generator from Dantec Dynamics that produced olive oil particles (0.5 μm). An air compressor was used to supply the seeding generator with compressed air. During the PIV measurements, the seeding generator was turned off. A calibration target with tiny dots formed a grid with dimensions of 100x100mm [24]. The size of each captured image was 250x250mm for the thermal plume and 380x380mm for the air jet. A FLIR E40 IR camera was used to measure the manikin's temperature gradient and evaluate the thermal plume around the head, using a thin metallic sheet with equidistant points 30 mm apart in the horizontal and vertical direction as a reference scale.

Fig. 2 – PIV calibration targets for air jet.

3. Numerical setup

Numerical simulation is widely used to study vehicle cabins' thermal and flow environments [7-9]. Based on this 1:1 scale cabin mock-up, the numerical model was designed and implemented in Ansys Fluent software (see Fig. 3).

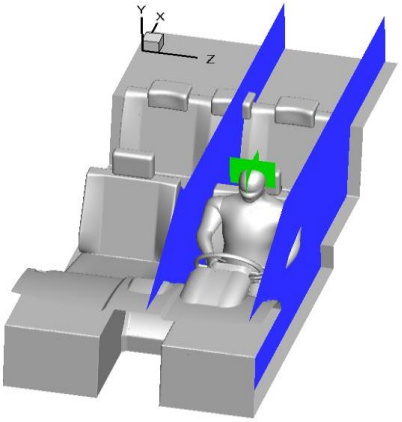

Fig. 3 – Side view of the studied geometrical model.

Steady-state RANS simulations were performed with the SST k-ω turbulence model. Different turbulence models in vehicle cabins were studied [20-21], advising the SST k-ω model for induced jet streams and the thermal plume [8]. For density models, ideal and incompressible-ideal gas and Boussinesq approximation were chosen and compared. The boundary conditions (BCs) for the manikin and the car cabin (windshield, front, ceiling, floor, rear window, left and right side) were set up with no-slip wall with a fixed temperature of 34°C and 20°C. The inlet BC of the air vents was set at 20°C and with an imposed mass flow rate of 0.0285 kg/s for the side air vents and 0.0354 kg/s for the central air vents based on experimental measurements and a constant turbulence intensity of 5% (see Tab. 1) being calculated using an empirical method [22]. We considered an isothermal uniform flow. As described in [22], the initial values of kinetic energy k, specific dissipation rate ω, and eddy viscosity ν_t were approximated. The governing equations were solved on a grid of polyhedral elements.

Tab. 1 – Calculation for Boundary conditions for air inlets.

	Left	Central left	Central right	Right
$\dot{m}$ [kg/s]	0.0136	0.0193	0.0161	0.0149
D_h [m]	0.076	0.074	0.074	0.076
Re	8273	11472	9422	9974
I [%]	5.2	5	5.1	5.1

Gradients were calculated with least-square-cell-based method. Coupled solver was chosen for pressure-velocity coupling scheme. Second-order upwind scheme was chosen to calculate the convective terms. The initialization was set to hybrid. Different meshes were considered and tested for the grid dependence test based on a previous study [14]. The CFD domain comprises 18 million polyhedral elements which, the boundary layer with prisms consists of 8 layers where the first cell height of 0.75mm and a growth factor of 1.2. Three refined mesh zones were created using the body influence technique as a critical area (see Fig 4).

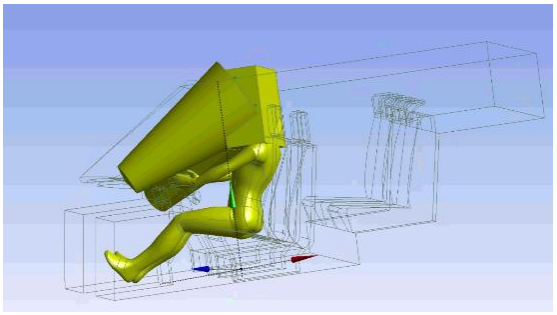

Fig. 4 – Mesh detail for the refining zones.

4. Results and discussion

Measurements and numerical simulations were performed in a full-scale passenger compartment considering only one HVAC volume flow rate (191.3 m^3/h). When comparing both results for the air velocity and temperature distributions in the sagittal and coronal planes (case 2), a good agreement was found regarding the ranges and distributions. An average correlation method to extract the velocity profiles was used for the PIV postprocessing in Dynamic Studio 7.2 software. Due to reflections, an image mask was defined to hide noisy vectors, such as vectors close to the Plexiglas roof or steering wheel.

4.1 Human thermal plume

Figures 5-12 present the thermal plume velocity and temperature distribution in sagittal and coronal planes. The thermal plume air and temperature distribution are asymmetrical in both cases. The flow structure in the car cabin is complicated with existing large- and small-scale vortices (See Fig. 13). For case 2, the thermal plume is stronger in front of the head, which is the opposite of case 1 back the head due to the following contributions. The airflow moves forward along the ceiling (see Fig. 13). The presence of the steering wheel distorts the flow direction at the thigh level (see Fig. 13). The additional velocity field on convective upward velocity in the shoulders' region is caused by impinging jets from diffusers. The Coanda effect caused by the central diffuser's flow creates a nonuniform and asymmetrical air distribution in the shoulders' region (see Fig. 13-14).

Tab. 2 – PIV/CFD comparison for velocity distribution.

V [m/s]	Sagittal		Coronal	
	PIV	CFD	PIV	CFD
Case 1	0.09-0.012		0.07-0.85	0.07-0.09
Case 2	0.15-0.2		0.12	0.12-0.15

The values determined in the sagittal and coronal planes for the temperature distribution of the thermal plume obtained by the numerical and experimental methods are very similar.
In both sagittal and coronal planes, the main upward-moving stream was observed, and the surrounding cold air flowed into the area that the hot plume left.
The thermal plume air and temperature distribution are also asymmetrical on the two measurement planes as previously.

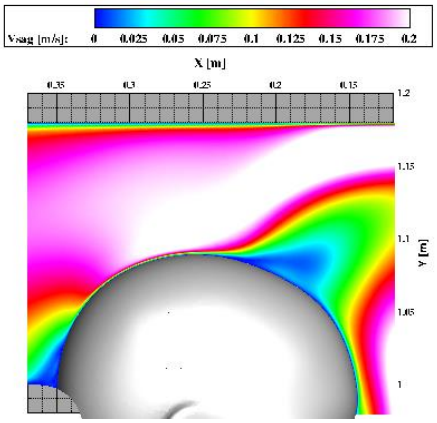

Fig. 5 – Thermal plume velocity distribution in sagittal plane (CFD).

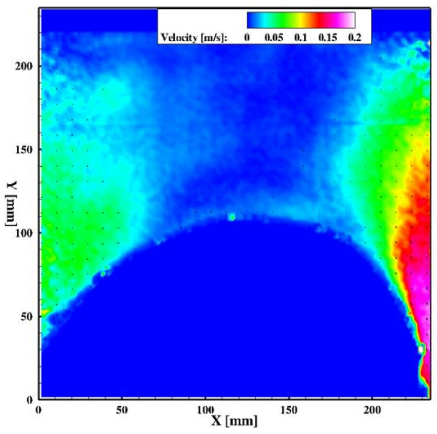

Fig. 6 – Thermal plume velocity distribution in sagittal plane (PIV).

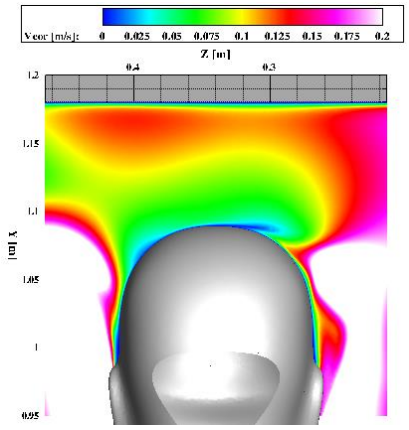

Fig. 7 – Thermal plume velocity distribution in coronal plane (CFD).

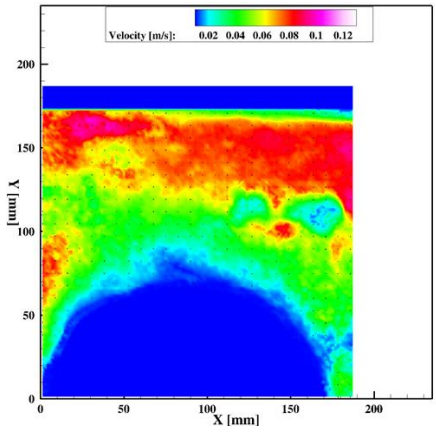

Fig. 8 – Thermal plume velocity distribution in coronal plane (PIV).

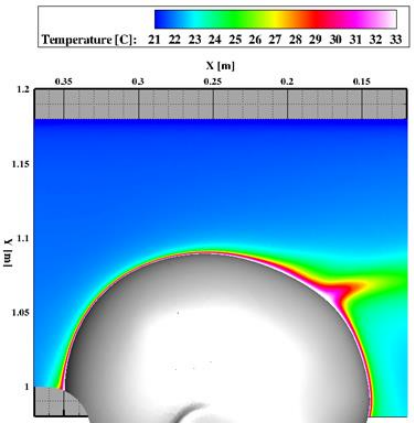

Fig. 9 – Thermal plume temperature distribution in sagittal plane (CFD).

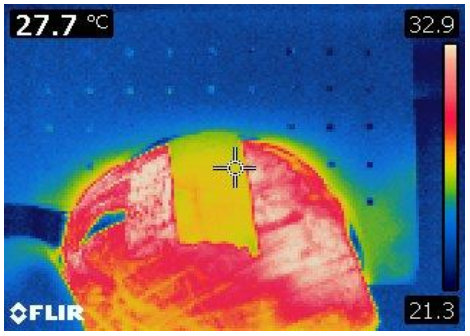

Fig. 10 – Thermal plume temperature distribution in sagittal plane (IR).

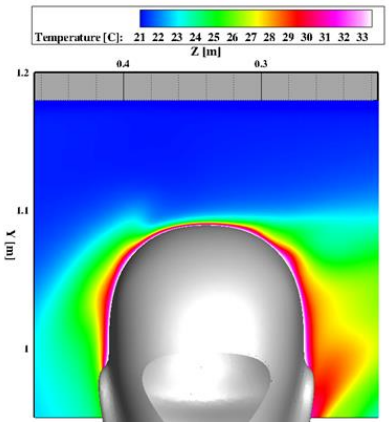

Fig. 11 – Thermal plume temperature distribution in coronal plane (CFD).

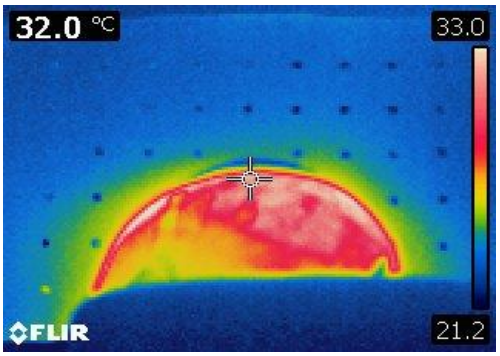

Fig. 12 – Thermal plume temperature distribution in the coronal plane (IR).

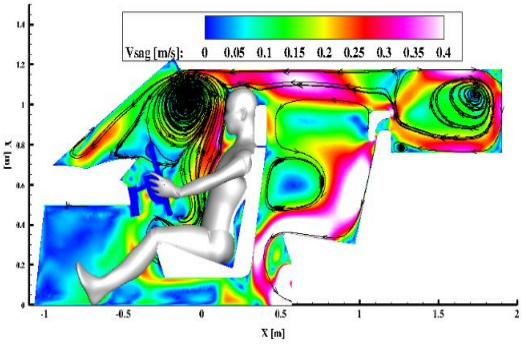

Fig. 13 – Velocity field in the driver's seat centre plane.

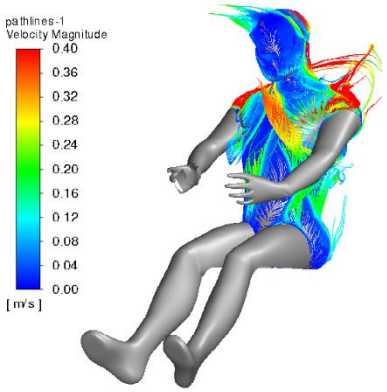

Fig. 14 – Pathlines showing the thermal plume on the manikin's body**.**

The distribution of the convective fluxes allows us to have a more precise idea of the thermal plume dynamics and heat transfer for each body's part. For case 2, a nonuniform and asymmetrical heat transfer can be observed (see Fig. 15).

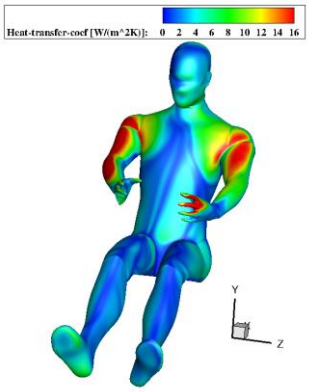

Fig. 15 – Convective heat flux on manikin surface.

4.2 Air jet

Figures 16-21 present the velocity distribution for CFD isothermal uniform flow and PIV measurements in the middle plane of the central left/ left side Classical Grilles (CG) and Lobed Aileron Grilles (LAG) diffusers. The results show that this qualitative comparison with PIV measurements is not too bad despite having a CFD isothermal uniform flow of air jets in terms of velocity range and the general shape of the jet stream. A disadvantage of this working assumption for the uniform flow is that the same velocity across the inlet area is an unrealistic situation. If a uniform air velocity is assumed as a BC, the airflow distribution in the cabin will change, and the passenger's thermal sensation will also change. PIV qualitative comparison of the jets' velocity distributions shows that with an innovative LAG diffuser, the velocities are more uniform than with the classical one since the flow injected through the lobed diffuser train more air and mix better with air from the cabin. This greater uniformity in the flows for LAG diffusers has been demonstrated in previous studies [25-26] with a critical value of 30^0 for the lobe inclination. If this critical value is not respected, there will be a separation of the two flows than the desired effect of mixing the two flows bounded by the sheet. It shows clearly the benefits of passive flow mixing to improve the thermal sensation.

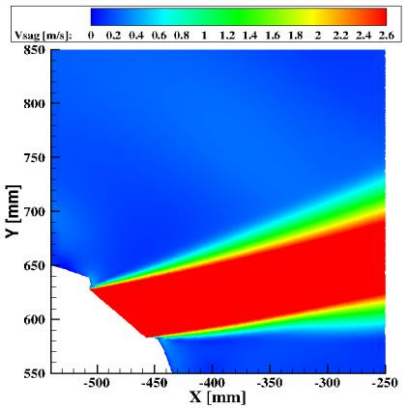

Fig. 16 – CFD velocity Distribution in the middle plane of the central left diffuser.

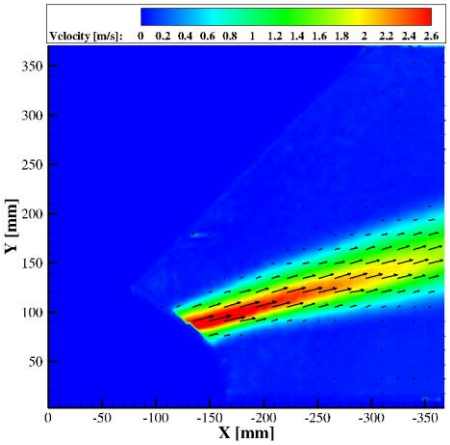

Fig. 17 – PIV velocity distribution in the middle plane of the central left CG diffuser.

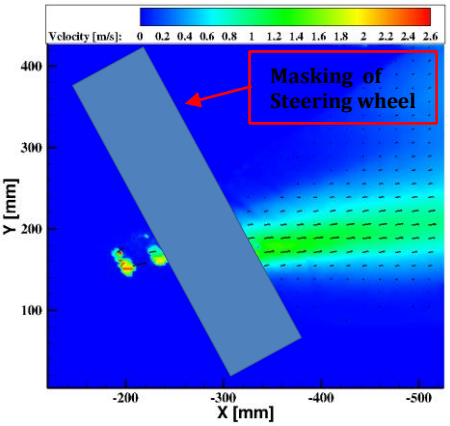

Fig. 18 – PIV velocity distribution in the middle plane of the central left LAG diffuser.

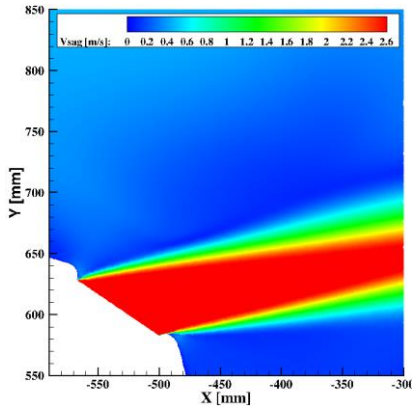

Fig. 19 – CFD velocity Distribution in the middle plane of the left side diffuser.

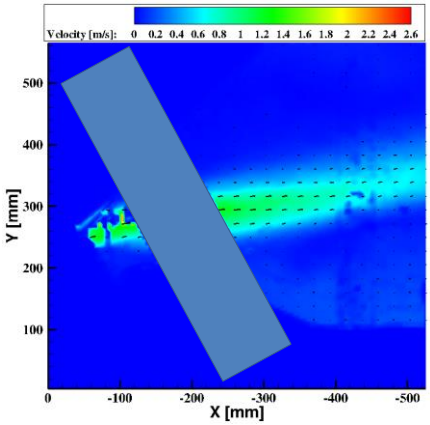

Fig. 20 – PIV velocity Distribution in the middle plane of the left side CG diffuser.

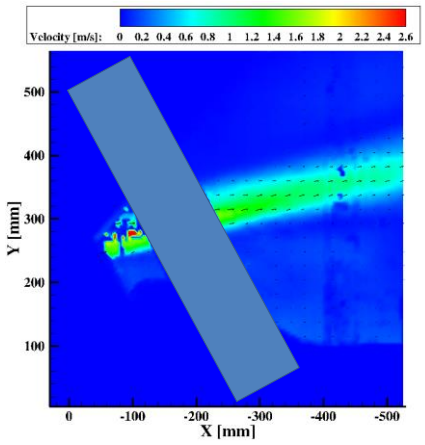

Fig. 21 – PIV velocity Distribution in the middle plane of the left side LAG diffuser.

5. Conclusion and perspectives

The results obtained by numerical and experimental methods showed good agreement regarding ranges and distributions in both planes for the thermal plume in case 2, where an isothermal uniform flow as CFD BC was used. The asymmetrical behaviour was observed in both planes for the thermal plume airflow and temperature distributions. The thermal plume is stronger in front of the head, which is the opposite of what was previously observed in the head [14] due to four different contributions, as explained in section 4.1.

To investigate thermal plume air distribution with PIV measurements, it is crucial to check the cabin's thermal equilibrium and the momentum of the seeding airflow.

A qualitative comparison of the jets' velocity distributions shows that with an innovative LAG diffuser, the velocities are more uniform than with the classical one since the flow injected through the lobed diffuser train more air and mix better with air from the cabin.

For future validations of this interaction, the next step will be to compare the PIV measurements for three different HVAC volume flow rates with two different approaches:

- Real 3D scanned ducts will be simulated separately from the car cabin to reduce computation time (see Fig. 22).
- BC's of air velocity distribution from LDV data.

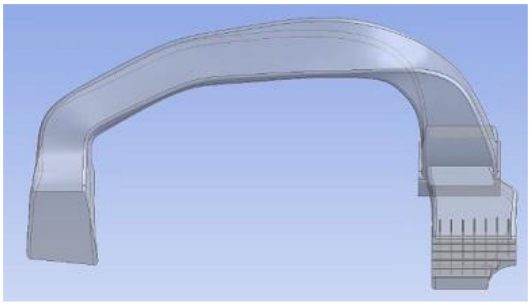

Fig. 22 – Geometry of real 3D scanned air ducts.

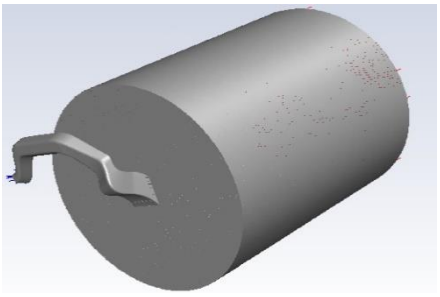

Fig. 23 – CFD domain of real 3D scanned air ducts.

6. Acknowledgement

This work was supported by a grant from the Romanian Ministry of Education and Research, CCCDI-UEFISCDI, project number PN-III-P2-2.1-PED-2019-4249, within PNCDI III, XTREME – Innovative system to extend the range of electric vehicle at improved thermal comfort.

7. Data access statement

Data sharing is not applicable to this article as no datasets were generated or analyzed during the

current study.

8. References

[1] Zhang B, Xue T, Hu N. Analysis and improvement of the comfort performance of a car's indoor environment based on the predicted mean vote–predicted percentage of dissatisfied and air age. Advances in Mechanical Engineering. 2017 Apr;9(4):1687814017695693.

[2] Croitoru C, Nastase I, Bode F, Meslem A, Dogeanu A. Thermal comfort models for indoor spaces and vehicles—Current capabilities and future perspectives. Renewable and Sustainable Energy Reviews. 2015 Apr 1;44:304-18.

[3] Zhang H, Dai L, Xu G, Li Y, Chen W, Tao W. Studies of airflow and temperature fields inside a passenger compartment for improving thermal comfort and saving energy. Part II: Simulation results and discussion. Applied Thermal Engineering. 2009 Jul 1;29(10):2028-36.

[4] Lee JP, Kim HL, Lee SJ. Large-scale PIV measurements of ventilation flow inside the passenger compartment of a real car. Journal of visualization. 2011 Dec;14(4):321-9.

[5] Mangili A, Gendreau MA. Transmission of infectious diseases during commercial air travel. The Lancet. 2005 Mar 12;365(9463):989-96.

[6] Kühn M, Bosbach J, Wagner C. Experimental parametric study of forced and mixed convection in a passenger aircraft cabin mock-up. Building and Environment. 2009 May 1;44(5):961-70.

[7] Bode F, Patrascu C, Nastase I. Heat and mass transfer enhancement strategies by impinging jets: A literature review. Thermal Science. 2021;25(4 Part A):2637-52.

[8] Amina M, Nastase I, Bode F, Beghein C. Optimization of a lobed perforated panel diffuser-a numerical study of orifice arrangement. International Journal of Ventilation. 2012 Dec 1;11(3):255-70.

[9] Nastase I, Meslem A, El Hassan M. Image processing analysis of vortex dynamics of lobed jets from three-dimensional diffusers. Fluid Dynamics Research. 2011 Nov 7;43(6):065502.

[10] Cao X, Liu J, Jiang N, Chen Q. Particle image velocimetry measurement of indoor airflow field: A review of the technologies and applications. Energy and Buildings. 2014 Feb 1:69:367-80.

[11] Cao X, Liu J, Pei J, Zhang Y, Li J, Zhu X. 2D-PIV measurement of aircraft cabin air distribution with a high spatial resolution. Building and Environment. 2014 Dec 1:82:9-19.

[12] Yang JH, Kato S, Nagano H. Measurement of Airflow of Air-Conditioning in a Car with PIV. Journal of visualization. 2009 Jun;12(2):119-30.

[13] Huera-Huarte FJ, Cort X, Aramburu E, Vizcaino X, Casto L. DPIV Measurements of the HVAC Aerodynamics Inside a Passenger Car. In23rd SAE Brasil International Congress and Display 2014 Sep 30 (No. 2014-36-0214).

[14] Jamin A, Janssens B, Bosschaerts W, Bode F, Danca PA, Nastase I. Experimental Validation of the Human Thermal Plume of the Driver Inside a Vehicle Cabin. In2021 10th International Conference on ENERGY and ENVIRONMENT (CIEM) 2021 Oct 14 (pp. 1-5). IEEE.

[15] Li J, Liu J, Wang C, Jiang N, Cao X. PIV methods for quantifying human thermal plumes in a cabin environment without ventilation. Journal of Visualization. 2017 Aug;20(3):535-48.

[16] Danca P, Bode F, Nastase I, Meslem A. CFD simulation of a cabin thermal environment with and without human body–thermal comfort evaluation. InE3S Web of Conferences 2018 (Vol. 32, p. 01018). EDP Sciences.

[17] Li J, Cao X, Liu J, Mohanarangam K, Yang W. PIV measurement of human thermal convection flow in a simplified vehicle cabin. Building and Environment. 2018 Oct 15;144:305-15.

[18] Li J, Liu J, Pei J, Mohanarangam K, Yang W. Experimental study of human thermal plumes in a small space via large-scale TR PIV system. International Journal of Heat and Mass Transfer. 2018 Dec 1;127:970-80.

[19] Ursu I, DG CC, Danca P, Nastase I. Advanced TMPrototype with Neurofuzzy Control System. COBEE 2018. 2018.

[20] Heider A, Konstantinov M, Lauenroth G, Rütten M, Werner F, Wagner C. Experimental and numerical investigations of cabinflow in a mini-van. In: Aero- dynamics of Heavy Vehicles III: Trucks, Buses and Trains (2010). https://elib.dlr. de/67185

[21] You R, Chen J, Shi Z, Liu W, Lin CH, Wei D, Chen Q. Experimental and numerical study of airflow distribution in an aircraft cabin mock-up with a gasper on. Journal of Building Performance Simulation. 2016 Sep 2;9(5):555-66.

[22] Jaramillo JE, Perez-Segarra CD, Rodriguez I, Oliva A. Numerical study of plane and round impinging jets using RANS models. Numerical Heat Transfer, Part B: Fundamentals. 2008 Aug 7;54(3):213-37.

[23] Ullrich S., Buder R., Boughanmi N., Friebe C., Wagner C. Numerical study of the airflow distribution in a passenger car cabin validated with PIV. In Symposium der Deutsche Gesellschaft für Luft-und Raumfahrt (pp. 457-467). Springer, Cham. 2018.

[24] Tacutu L, Bode F, Năstase I, Croitoru C, Dogeanu A. Experimental and numerical study on the thermal plumes of a standing and lying human in an operating room. Science and Technology for the Built Environment. 2022 Jan 2;28(1):2-0.

[25] O'sullivan M. N., Krasnodebski J. K., Waitz I. A., Greitzer E. M., Tan C. S., & Dawes W. N. Computational study of viscous effects on lobed mixer flow features and performance. Journal of Propulsion and Power, 1996, 12(3), 449-456.

[26] NASTASE I. Analyse des jets lobés en vue de leur intégration dans les Unités Terminales de Diffusion d'air. 2007. Thèse de doctorat. La Rochelle.